Eur. Phys. J. B **16**, 147–155 (2000)

THE EUROPEAN PHYSICAL JOURNAL B

EDP Sciences

Spike-burst and other oscillations in a system composed of two coupled, drastically different elements

V.I. Nekorkin[1,2], V.B. Kazantsev[1], and M.G. Velarde[2,a]

[1] Radiophysical Department, Nizhny Novgorod State University 23 Gagarin Ave., 603600 Nizhny Novgorod, Russia
[2] Instituto Pluridisciplinar, Universidad Complutense, Paseo Juan XXIII, N° 1, Madrid 28 040, Spain

Received 19 March 1999 and Received in final form 1 November 1999

Abstract. The dynamics of a system composed of two nonlinearly coupled, drastically different nonlinear and eventually oscillatory elements is studied. The rich variety of attractors of the system is studied with the help of phase space analysis and Poincare maps.

PACS. 05.45.-a Nonlinear dynamics and nonlinear dynamical systems

1 Introduction

Systems composed of two or several coupled oscillatory components or elements are useful when modeling nonlinear processes in many areas of science [1–9]. One of the oscillators may exhibit quasiharmonic oscillations yet nonlinear with definite amplitude and frequency, relaxation-like oscillations with definite period or time-chaotic oscillations. Other components may simply be excitable nonlinear elements in the ensemble. The collective dynamics of such an assembly is determined by both the dynamics of the components and the type of coupling between them. Such composite systems may be useful models or building blocks for chemical and biochemical processes [1–4], in physiology [5–9] or in electronics [10,11]. Thus in the perspective of such possible wide applicability it seems worth to explore the dynamical behavior and attractors, and hence the physical properties of a system composed of two drastically different nonlinear elements coupled by also nonlinear functions. For illustration we consider a Van der Pol oscillator exhibiting (nonlinear) quasiharmonic oscillations and a FitzHugh-Nagumo system displaying relaxation-like behavior. We show that such system with the two parts responsible for really different functions allows a rich variety of oscillatory and complex chaotic modes.

Note that although a harmonic oscillator is capable of accounting for quasiharmonic oscillations yet it is of no use to our purpose as we would like to have an oscillator whose amplitude and frequency do not depend on initial conditions (*i.e.* a limit cycle). On the other hand, the choice of a FitzHugh-Nagumo excitable element and a Van der Pol oscillator and not two coupled Van der Pol oscillators, say, one quasiharmonic and the other in the relaxational regime is dictated by our interest of clearly separating a relaxational, non-oscillatory evolution from the time oscillatory (limit cycle) regime.

In Section 2 we define the model-problem to be studied. Section 3 is devoted to the analysis of various oscillatory and relaxational regimes of the chosen composite system. In Section 4 we deal with chaotic oscillations. Finally, in Section 5 we provide some conclusions.

2 Model

Let us construct two building blocks possessing the following two characteristics, taken separately

(i) one exhibits quasiharmonic oscillations;
(ii) the other incorporates an excitation threshold above which short powerful, hence relaxation-like pulses are emitted.

An oscillator found in many realms of science satisfying condition (i) is the Van der Pol oscillator (VdP) defined by the equations

$$\begin{cases} \dfrac{\mathrm{d}x}{\mathrm{d}t} = y \\ \dfrac{\mathrm{d}y}{\mathrm{d}t} = \mu(\gamma - x^2)y - \omega^2 x, \end{cases} \tag{1}$$

where $\mu \ll 1$ is a small parameter and ω gives the oscillation frequency. When $\gamma = 0$ the system (1) displays a supercritical Andronov-Hopf bifurcation [12] and for $\gamma > 0$ a limit cycle appears in its phase plane.

A system capable of relaxation-like pulse generation as demanded with condition (ii) is the FitzHugh-Nagumo model (FHN)in the form [13]

$$\begin{cases} \dfrac{\mathrm{d}u}{\mathrm{d}t} = f(u) - v \\ \dfrac{\mathrm{d}v}{\mathrm{d}t} = \varepsilon(u - b), \end{cases} \tag{2}$$

[a] e-mail: mvelarde@pluri.ucm.es

where $f(u)$ is the nonlinear function of cubic or sigmoidal shape, ε is a smallness parameter, $0 < \varepsilon \ll 1$, and b is a parameter driving the excitation threshold. When exceeding the excitation threshold (for example, by applying an external perturbation that could be provided by the Van der Pol element (1)) there arises the relaxation-like pulse. Then the system returns back to the original rest state given by the single stable fixed point. Note, that in equations (2) the fast variable u is like a chemical activator, and v is responsible for "recovering" the rest state as an inhibitor [3,4].

A composite dynamical system possessing together the two features, (i) and (ii), just described can be obtained by coupling (1) to (2). We set

$$\begin{cases} \varepsilon_1 \dfrac{\mathrm{d}u}{\mathrm{d}t} = f(u) - v - y, \\ \dfrac{\mathrm{d}v}{\mathrm{d}t} = \varepsilon_2(u + I), \\ \dfrac{\mathrm{d}x}{\mathrm{d}t} = y, \\ \dfrac{\mathrm{d}y}{\mathrm{d}t} = (\Gamma(u, I) - lx^2)y - \Omega(u, I)x, \end{cases} \tag{3}$$

where the variables of the FHN component, (u, v), describe the pulse generation and the VdP variables, (x, y), describe the rhythm of the limit cycle oscillations. Note, that if we wish the composite system to be endowed with more than one excitability threshold it suffices to add another FHN excitable element or some other equivalent component. The parameter I plays the role of external stimulus; l characterizes the robustness of the oscillations ($l = 0$ corresponds to a harmonic oscillator) and $0 < \varepsilon_1 \ll 1$. The functions $\Gamma(u, I)$ and $\Omega(u, I)$ change the amplitude and frequency of the oscillations depending on the values taken by u and on the values of the external stimulus, I. Their concrete forms will be discussed later in accordance to the specific dynamical behavior we would like to have. The second smallness parameter, $0 < \varepsilon_2 \ll 1$, allows to tune, separately or simultaneously, the characteristic time scales of the relaxation-like pulse of equations (2) and the oscillations of equations (1).

3 Quasiharmonic and relaxational oscillations

Following [13], we take $f(u)$ in the piece-wise linear form

$$f(u) = \begin{cases} -m_1 u, & \text{if } u \le a, \\ m_2 u - a(m_1 + m_2) & \text{if } a < u < 1, \\ -m_3 u - a(m_1 + m_2) + m_3 + m_2 & \text{if } u \ge 1. \end{cases}$$

with a, m_1, m_2, $m_3 > 0$, (4)

and for the coupling functions Γ and Ω we start taking rather simple forms. Then, system (3) reduces to

$$\begin{cases} \varepsilon_1 \dfrac{\mathrm{d}u}{\mathrm{d}t} = f(u) - v - y, \\ \dfrac{\mathrm{d}v}{\mathrm{d}t} = \varepsilon_2(u + I), \\ \dfrac{\mathrm{d}x}{\mathrm{d}t} = y, \\ \dfrac{\mathrm{d}y}{\mathrm{d}t} = (\gamma(1 + \alpha I + \beta u) - lx^2)y - \omega_0^2 x, \end{cases} \tag{5}$$

with $\gamma, \beta > 0$ and $\alpha < 0$ fixed coefficients.

3.1 Phase space analysis

Let us denote by G the four-dimensional phase space of system (5).

3.1.1 Fast motions of the system (5)

Let us consider the surface $\mathrm{F} = \{f(u) - v - y = 0\}$ in the phase space G. This surface is an integral manifold of system (5) in the case $\varepsilon_1 = 0$. It represents a Z-shaped surface. When $\varepsilon_1 \to 0$, the variable u changes rapidly, $\dot{u} \to \infty$, outside the surface F, while the other variables change with a finite velocity. Therefore, when $\varepsilon_1 \to 0$, all trajectories of system (5) belong to the planes

$$v, x, y = \text{const.} \tag{6}$$

Along these planes the trajectories evolve with an arbitrary high rate of change in u ($\varepsilon_1 \to 0$). Hence, they correspond to "fast" motions of the system [12,14] which are approximately described by the equation

$$\varepsilon_1 \dot{u} = f(u) - v^0 - y^0, \tag{7}$$

with $v^0, y^0 = \text{const}$. To simplify notation a dot accounts for time derivative.

3.1.2 Slow motions of system (5)

It follows from (7) that all fast motions of system (5) asymptotically tend to those parts of the surface F where the inequality $f'(u) < 0$ is satisfied. Taking into account (4) we find that there exist two regions of the surface F which attract all fast motions. We denote them by F_0^+ and F_1^+,

$$\begin{cases} \mathrm{F}_0^+ = \{f(u) - v - y = 0, \quad u < a\} \\ \mathrm{F}_1^+ = \{f(u) - v - y = 0, \quad u > 1\}. \end{cases} \tag{8}$$

In the corresponding neighborhoods (order ε_1) of the regions F_0^+ and F_1^+ the trajectories of system (5) evolve with velocities bounded on each variable. These are the "slow"

motions [12,14]. With accuracy up to terms of higher order the slow motions are described by the reduced system

$$\begin{cases} \dot{v} = \varepsilon_2(u + I), \\ \dot{x} = y, \\ \dot{y} = (\gamma(1 + \alpha I + \beta u) - lx^2)y - \omega_0^2 x, \\ f(u) - v - y = 0. \end{cases} \tag{9}$$

For simplicity, we take $m_1 = m_3 = 1$. In this case the slow motions in the neighborhoods of F_0^+ and F_1^+ are governed by the same system which can be written in the form

$$\begin{cases} \dot{x} = y, \\ \dot{y} = \Phi(x, y, z)y - \omega_0^2 x, \\ \dot{z} = -\varepsilon_2(z - y + I), \end{cases} \tag{10}$$

where

$$z \equiv u + y, \qquad \Phi(x, y, z) \equiv \gamma[1 + \alpha I + \beta u] - lx^2.$$

Thus, the trajectories of the system (5) have both fast and slow features. Generally, this allows two basic attractors:

(i) Attractors entirely located within the neighborhoods of the regions F_0^+ and F_1^+. Such attractors have no fast motions.
(ii) Attractors which have both fast and slow parts of motions.

3.1.3 Jumps of the variable z

In the attractors of type (ii) the parts of slow motions sequentially change with very rapid (instantaneous) jumps of the variable u. It follows from (7) that these jumps occur at the planes $\{u = a\}$ and $\{u = 1\}$. Let us denote by G^+ the phase space of system (10). Then, in G^+ these planes correspond to the planes

$$Z_a = \{z - y = a\}, \text{and } \; Z_1 = \{z - y = 1\}, \tag{11}$$

respectively. Note, that in the phase space G^+ the region F_0^+ lies below the plane Z_a, while F_1^+ lies above the plane Z_1. The fast motions of system (5) make "connections" between the trajectories of both regions, F_0^+ and F_1^+. Since outside the small neighborhoods of F_0^+ and F_1^+ the inequality (6) is fulfilled, the fast motions can be approximately taken into account with instant jumps of the variable z. Let $x = x^-, y = y^-, z = z^-$ be the coordinates of a phase space point before the jump, and $x = x^+, y = y^+, z = z^+$ define the point after the jump. Using (6) we find from (8) the following jump rules

$$\begin{aligned} &x^+ = x^-, \;\; y^+ = y^-, \;\; z^+ = z^- + (1 + m_2)(1 - a) \\ &\qquad\qquad \text{if } (x^-, y^-, z^-) \in Z_a; \\ &x^+ = x^-, \;\; y^+ = y^-, \;\; z^+ = z^- - (1 + m_2)(1 - a) \\ &\qquad\qquad \text{if } (x^-, y^-, z^-) \in Z_1. \end{aligned} \tag{12}$$

Let us now find the attractors of the system (5).

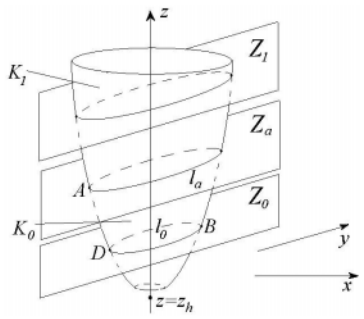

Fig. 1. A qualitative view of the phase space G of the system (5). K_0 is the *slow* motion surface. The planes Z_a, Z_1 are switch-planes. When trajectories hit the planes they jump with *fast* motions.

3.2 Quasiharmonic oscillations

Consider the slow motions (10) when $\varepsilon_2 \to 0$. In this case each plane $\{z = z_0 = \text{const}\}$ in the phase space G^+ represents an integral manifold. Motions on the plane $\{z = z_0\}$ are governed by the system

$$\begin{cases} \dot{x} = y, \\ \dot{y} = [\gamma(1 + \alpha I + \beta z_0 - \beta y) - lx^2]y - \omega_0^2 x. \end{cases} \tag{13}$$

The system (13) has a single steady point at the origin, $O(0, 0)$. This point is stable if $z_0 < z_h$, $z_h \equiv -(1 + \alpha I)/\beta$ and otherwise it is unstable. It can be shown that the fixed point $O(0, 0)$ loses the stability by a supercritical Andronov-Hopf bifurcation. Then, on each plane $z = z_0$, for $z_0 > z_h$, the system (13) has a stable limit cycle. Let us denote this cycle by $C(z_0)$. Increasing z_0, from $z_0 = z_h$, the size (amplitude) of the limit cycle $C(z_0)$ monotonically increases. In the phase space G^+ the cycle $C(z_0)$ forms a conical surface with apex at $(0, 0, z_h)$. We denote this surface by $K(0)$. Note, that using the averaging procedure [15,16] for $\gamma = \mu\tilde{\gamma}$ and $l = \mu\tilde{l}$, with $\mu \ll 1$, one can show that the surface $K(0)$ approaches

$$x^2 + \frac{y^2}{\omega_0^2} = \frac{4\tilde{\gamma}}{\tilde{l}}\left[1 + (\alpha - \beta)I + \beta z_0\right]. \tag{14}$$

Let us take now ε_2 sufficiently small, $0 < \varepsilon_2 \ll 1$. Then, from the theory of continuous dependence of integral manifolds on a parameter [17,18] follows that an integral manifold $K(\varepsilon_2)$ exists in the system (10). The manifold $K(\varepsilon_2)$ exists for $z > z_h + z^0$, where the infinitesimally small parameter $z^0(\varepsilon_2)$ satisfies the conditions $z^0 > 0$, and $\lim_{\varepsilon_2 \to 0} z^0(\varepsilon_2) = 0$. Then, $K(\varepsilon_2) \to K(0)$ with $\varepsilon_2 \to 0$. The qualitative shape of the surface $K(\varepsilon_2)$ is shown in Figure 1a. Note, that the surface $K(\varepsilon_2)$ is defined only in the regions F_0^+ and F_1^+ of the phase space. Therefore, only those parts of $K(\varepsilon_2)$ located below the plane Z_a and above the plane Z_1 are defined in the phase space G^+ (Fig. 1). We denote these parts by K_1 and K_0, respectively.

Let us show that there is a set of parameter values for which the system (10) has a stable limit cycle in K_0. The cycle "embraces" the surface K_0. Consider the plane

$$Z_0 = \{z - y + I = 0\} \cdot$$

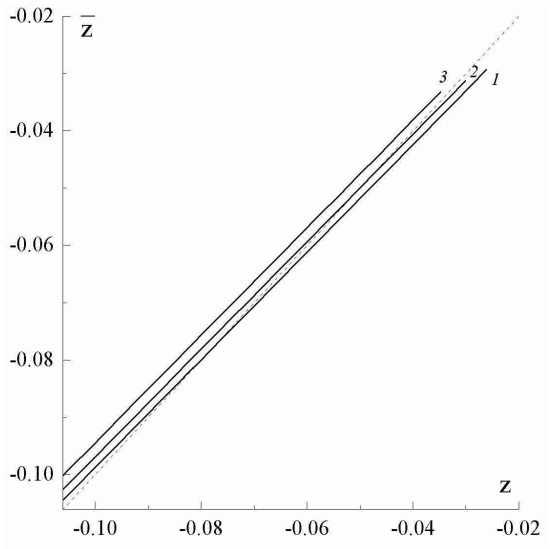

Fig. 2. Poincaré return map describing motions on the manifold K_0^+. The fixed point corresponds to the stable limit cycle C_0 and the quasiharmonic oscillations. Parameter values: $\alpha = -5, \beta = 5, \gamma = 0.001, l = 2, m_2 = 0.1$. Curve "1": $I = 0.08$, curve "2": $I = 0.05$, curve "3": $I = 0.01$. In case "3" there is no fixed point and trajectories transitively go up to the switch plane Z_a.

It follows from (10) that $\dot{z} = 0$ on this plane, $\dot{z} < 0$ above the plane, and $\dot{z} > 0$ below the plane. The planes Z_a and Z_0 intersect the surface K_0 at some elliptic curves, l_a and l_0,

$$l_a = K_0 \cap Z_a \quad \text{and} \quad l_0 = K_0 \cap Z_0, \tag{15}$$

respectively (Fig. 1). Let A be the point of the curve l_a where the variable z at l_a takes its minimum. We call it $z = z_A$. Let B and D be the points of l_0 where z at l_0 take minimal and maximal values. We call them $z = z_B$ and $z = z_D$, respectively (Fig. 1). Let us choose the parameters of the system (10) satisfying the inequality $z_A > z_D$. Call K_0^+ the part of the surface K_0 which is located between the curves

$$l_B = K_0 \cap \{z = z_B\} \qquad l_D = K_0 \cap \{z = z_D\}\,.$$

From the third equation in (10) follows that the trajectories of the system (10), belonging to K_0, intersect the curves l_B and l_D inward to K_0^+. Then, the system (10) does not have steady points in K_0^+. Therefore, in K_0^+ the Poincaré return map is

$$z \to g(z), \tag{16}$$

with $z \in L = K_0^+ \cap \{x = 0\}$. The map (16) has been numerically obtained (Fig. 2). It has a single stable fixed point which corresponds to a stable limit cycle C_0 in system (10) embracing K_0. Hence, a stable limit cycle C_0 formed by slow motions exists in the phase space G of system (5). The three solid curves correspond to different values of the control parameter I. Increasing I, the fixed point moves up and hence the limit cycle climbs up on the surface K_0^+. The third map curve, $I = 0.01$, does not have a fixed point. In this case the trajectories reach the switch plane Z_a and leave the surface K_0^+. The system (5) does not have limit cycles on the integral manifold. The attractors of the system in this case are studied in the next subsection. Note, that the map curves are close to the diagonal, *i.e.* $g'(z) \to 1$, with the prime denoting the corresponding z-derivative. Then, the approach to the fixed point proceeds very slow. This is because $\varepsilon_2 \to 0$ and the trajectories of the system (5) evolve slowly along the variable z in the phase space G^+.

Figure 3 illustrates the evolution of $u(t)$ as quasiharmonic oscillations of the model (5) (Fig. 3a) and the projection of C_0 on the plane (x, y) (Fig. 3b).

3.3 Relaxation-like limit cycles

Although for suitable parameter values the VdP alone is capable of exhibiting either quasiharmonic or relaxation limit cycles, we restrict consideration to the former only. We would like to have relaxation-like pulses on top of these oscillations [5,7–9]. Accordingly, in this subsection we continue the study of the dynamical properties of (5), which is the chosen particular case of the composite (3) with rather simple Γ and Ω feedback functions.

Let us decrease the control parameter I. In this case the plane Z_0 approaches the plane Z_a in the phase space G^+ (Fig. 1). Since the limit cycle C_0 on K_0^+ located between the curves l_B and l_D intersects Z_0, then C_0 is also climbing up to K_0 when I decreases. There is a critical value, $I = I_0$, when the cycle C_0 touches the plane Z_a. It breaks the cycle C_0. Let us show that in this case an attractor of type (ii) (Sect. A) appears in the phase space G of system (5). Its trajectories have both fast and slow features.

3.3.1 Poincaré map

Let $s_0(x_0, y_0, z_0)$ be a point of the plane Z_a belonging to an ε-neighborhood ($0 < \varepsilon \ll 1$) of the curve l_a (see (15) and Fig. 1). Consider the behavior of the trajectory, S, of system (3) crossing this point. Motions along S can be divided into four components.

1. Moving *fast* the variable z makes a jump with negligible changes of the other variables, x, y (Sect. A). Using (12) we find that after the jump the phase point at S has the coordinates

$$x \approx x_0, \quad y \approx y_0, \quad z \approx z_0 + (1 + m_2)(1 - a). \tag{17}$$

We denote this point by s_0. Then, $s_0 \in G_1 = G^+ \cap \{z - y > 1\}$, *i.e.* the point s_0 is located above the plane Z_1 (Fig. 1).

2. Leaving s_0 the trajectory S moves *slowly* in the neighborhood of K_1 (Fig. 1). Since $\dot{z} < 0$ for all points of the region G_1 after some time S comes to the plane Z_1 and hence leaves the region G_1 (Fig. 1). Let $s_1(x_1, y_1, z_1)$ be the intersection point of S and Z_1.

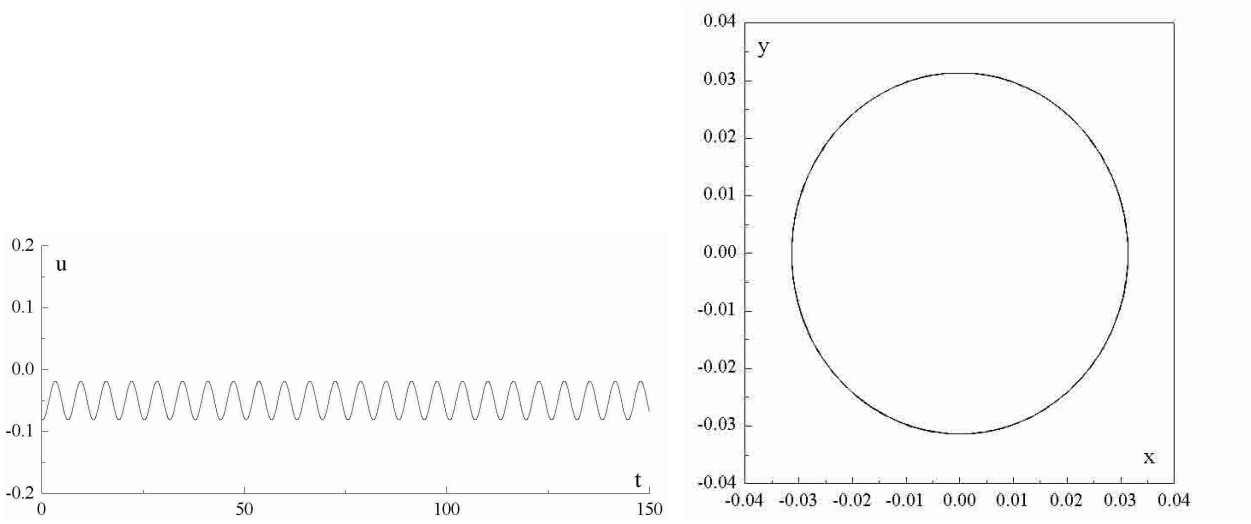

(a) (b)

Fig. 3. Quasiharmonic oscillations corresponding to the limit cycle C_0 on the manifold K_0^+. Time realizations of variable $u(t)$, and corresponding phase trajectories in the plane (x, u) of the model (5). Parameter values: $\alpha = -5, \beta = 5, \gamma = 0.001, l = 2, m_2 = 0.1, I = 0.05$.

3. At the point s_1 the trajectory S falls down along the variable z with negligible changes of x, y according to (12). Then, the coordinates of the phase point at S are

$$x \approx x_1, \quad y \approx y_1, \quad z \approx z_1 - (1 + m_2)(1 - a). \qquad (18)$$

We denote this point by s_a. Then, $s_a \in G_a = G^+ \cap \{z - y < a\}$, *i.e.* the point s_a is located below the plane Z_a in the phase space G^+ of system (10). Note, that Z_0 divides G_a into two parts, $G_a^+ = G_a \cap \{z - y + I < 0\}$ and $G_a^- = G_a \cap \{z - y + I > 0\}$.

4. Leaving the point s_a the trajectory S proceeds with *slow* motions of (10) near the surface K_0. Let us choose the value of I such that $z_B > z_A$ and $s_a \in G_a^+$ (Fig. 1). Then, past the point s_a, the trajectory S climbs up because in this region, G_a^+, the inequality $\dot{z} > 0$ is satisfied. During this process the trajectory S makes a number of oscillations around K_0. The variable z increases value at S until the trajectory intersects the plane Z_0. At all points above Z_0 the variable z is slowly decreasing. Thus, S intersects twice the plane Z_0 during one oscillation. Then, for suitable parameter values the trajectory S on the "average" in a single turn around K_0 still goes up until it intersects the switch plane Z_a at some point $\bar{s}(\bar{x}, \bar{y}, \bar{z})$. Note, that if $a < -I < 1$ the region G_a^- does not exist and the variable z grows monotonically from the point s_a to the point $\bar{s}$. Hence, there is a Poincaré return map

$$s \to \bar{s} = \Pi(s).$$

It is a two-dimensional map because the coordinates z and y are linked by the equation defining the plane Z_a. However, for a particular choice of parameter values (for instance, if l is large enough) there is rather strong compression to the surface K_0. Then, if we choose the initial point s on the line l_a, the point $\bar{s}$ approaches the line l_a and the Poincaré return map Π becomes quasi–one-dimensional.

3.4 Attractors of the map Π

Let us construct Poincaré return maps for the attractors of the second type (ii) involving both *fast* and *slow* motions of the system (5). For illustration we fix the parameters to the particular values $\alpha = -5, \beta = 5, \gamma = 0.001, l = 2, m_2 = 0.1$. This set allows us to characterize motions by using the one-dimensional map Π. We set the control parameter I such that the plane Z_0 stays above Z_a. This ensures the inequality $z_A > z_D$, and hence the trajectory surely leaves the surface K_0^+ and has *fast* motions. We vary the initial point s along the elliptic curve l_a, then the return point $\bar{s}$ tends to l_a and, hence the map Π is indeed one-dimensional. Figure 4a illustrates the map Π in the plane (x, y). The solid curve is mapped by the system (10) with jumps (12) into the curve labeled by circles which is rather close to l_a. To describe the behavior of the map we follow the x–coordinate of s, *i.e.* the map Π is g: $x \to \bar{x}$.

Figure 4b illustrates the map Π when it has a single stable fixed point. This point defines stable relaxation-like limit cycle behavior in the phase space G. The time realization of $u(t)$ and the phase portrait of the attractor in the plane (u, x) are shown in Figure 5. Such an attractor describes the *threshold* mode of the system when it generates pulses over the smooth limit cycle oscillatory rythm. In this case when the trajectory reaches the threshold (Z_a), up and down jumps (spikes) of u occur. Subsequently, the trajectory returns back to the quasiharmonic mode.

There are other relaxation-like attractors and threshold oscillations when Π does not have a simple (period one) fixed point (Fig. 6). For instance, the map may consist of a few continuous parts and a more complex (multiple period) periodic cycle appears in the phase space G of (5). Figures 7a, b illustrate the time realization $u(t)$

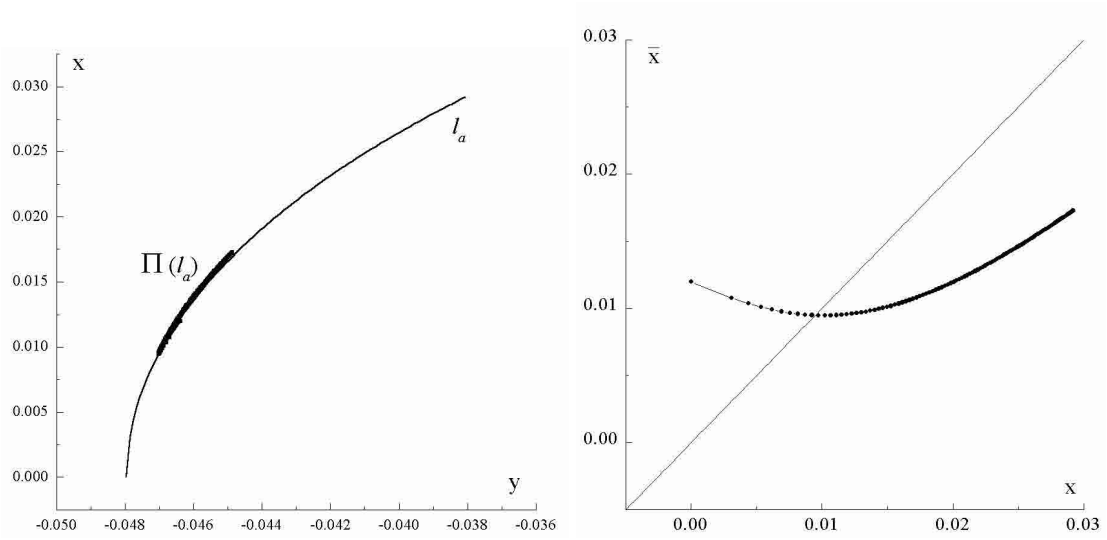

Fig. 4. Map Π describing a relaxation-like limit cycle. $I = -0.02$. (a) Map Π in the plane (x, y). The solid curve accounts for the initial points s on the line l_a. The curve labeled with circles is the transformation of l_a with the flow (3). (b) The dependence of the mapped point $\bar{x}$ on the initial point x of map Π. There is one stable fixed point corresponding to the cycle.

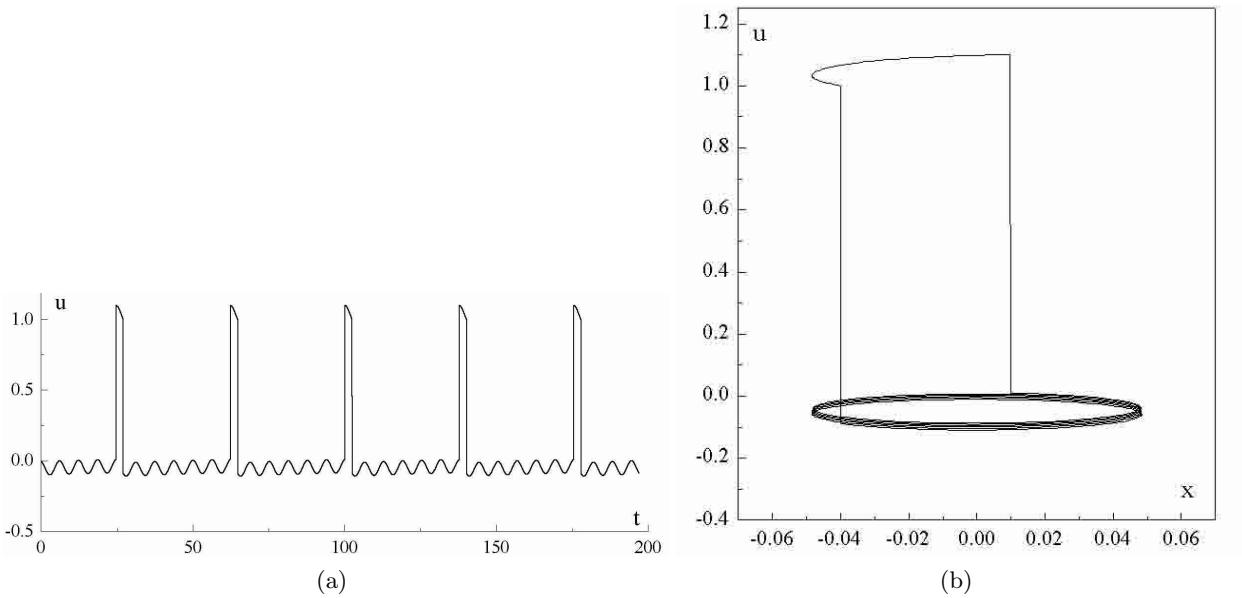

Fig. 5. Relaxation-like limit cycle. (a) Time realizations of variable $u(t)$, and (b) corresponding phase trajectories in the plane (x, u) of the model (5). $I = -0.02$.

and phase portrait of the cycle defined by the map. This limit cycle is of period 4. Note, that here the spikes appear with different inter-spike intervals. These differences in the inter-spike interval are one (or more) periods of the quasiharmonic oscillations. Note that the spikes occur only at maxima of the quasiharmonic oscillations. Each continuous part of the map Π (Fig. 6b) corresponds to a definite value of the inter-spike interval.

Note, that the one-dimensional map obtained for multiple period limit cycles (Fig. 6b) gives a rather rough approximation to the actual trajectory (Fig. 7a) in the three-dimensional phase space. However, it allows to estimate the shape of the actual map curve for correction of the map to match map trajectories and trajectories of the original system (10). In particular, in the case of Figure 6 where the map has three continuous parts

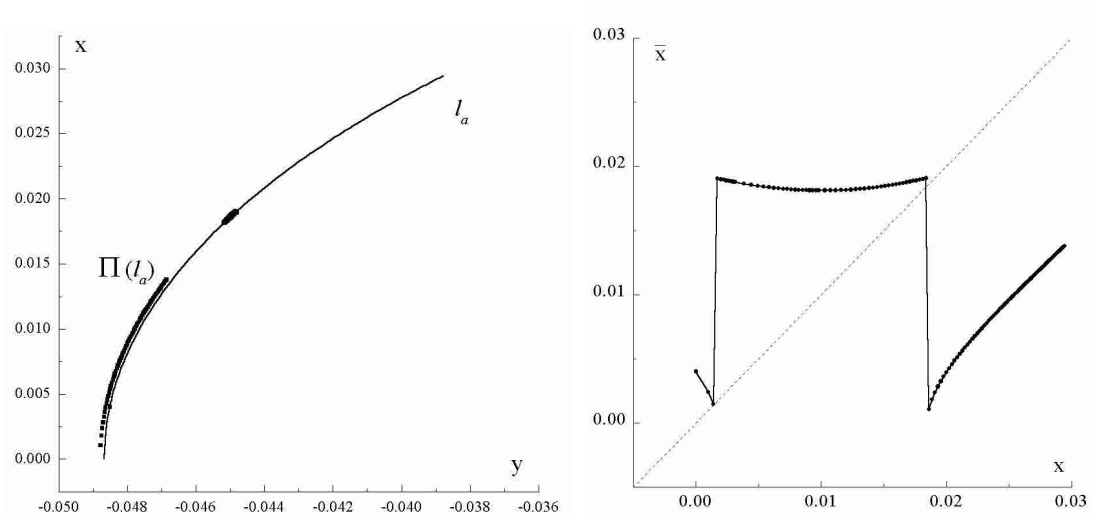

(a) (b)

Fig. 6. Map Π describing relaxation-like limit cycle of multiple period. $I = -0.027$. (a) Transformation of l_a under map Π in the plane (x, y). (b) The dependence of the mapped point $\bar{x}$ on the initial point x of map Π. There is no fixed point of period one. Each continuous part of the map corresponds to a definite time interval (inter-spike interval) between two consecutive spikes.

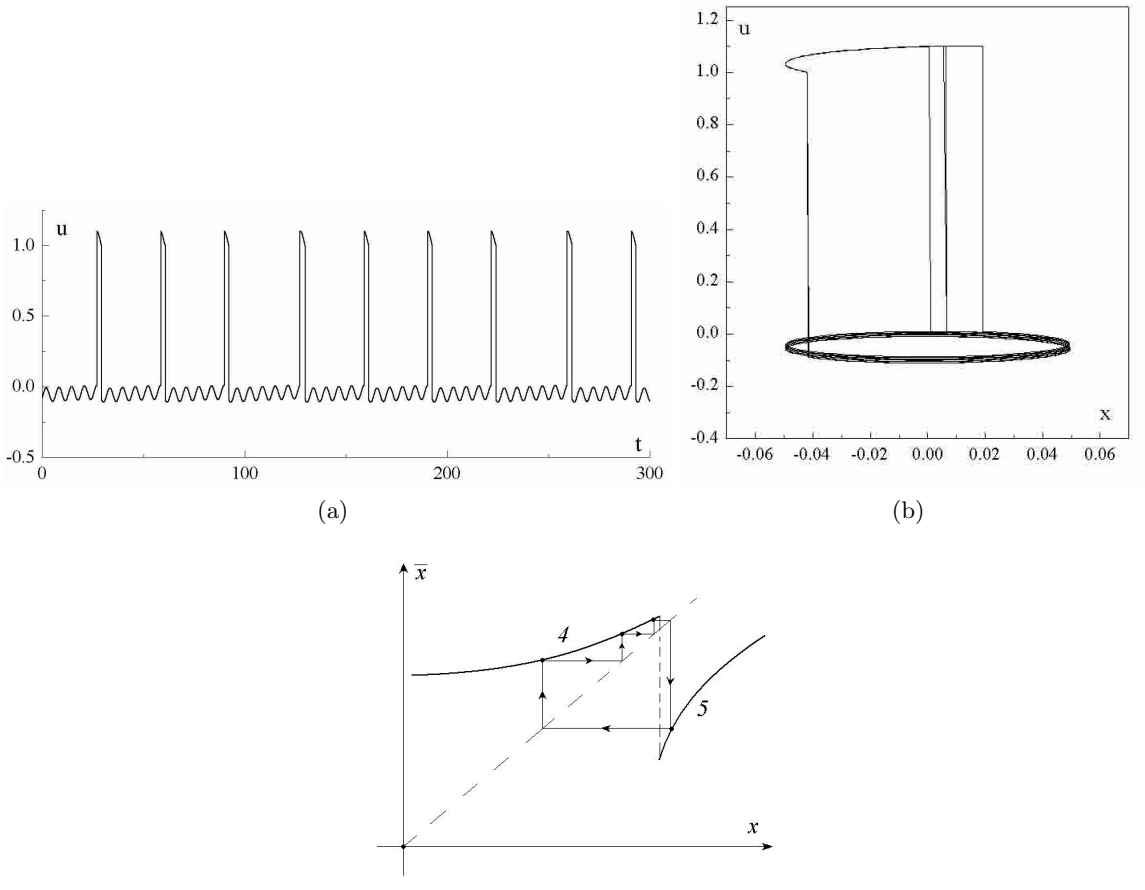

(a) (b)

(c)

Fig. 7. (a) Time realizations of $u(t)$ corresponding to the map of Figure 6. (b) Phase trajectories in the plane (x, u) of the model (5). $I = -0.027$. (c) Qualitative shape of the corrected map to describe multiple period attractors.

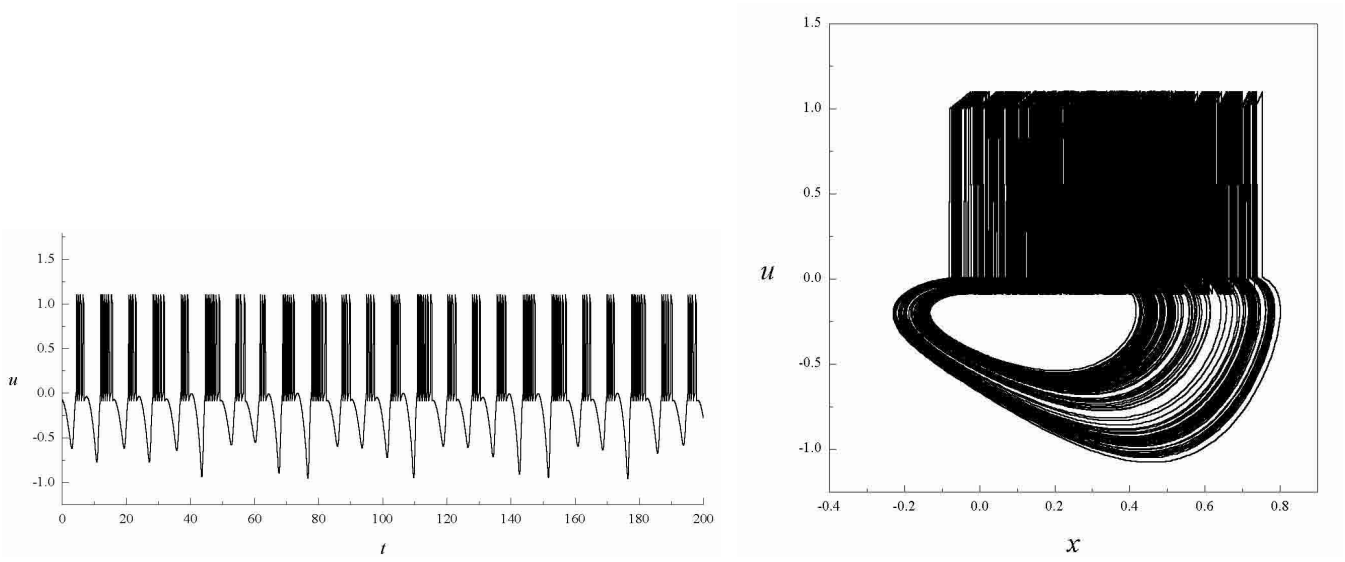

(a) (b)

Fig. 8. Spike-burst behavior exhibited by oscillator (3) for a suitable choice of the parameter values and coupling functions. (a) Time realization $u(t)$. (b) A view of the attractor in (x, u) representation.

it can be done as follows. The right continuous part corresponds to 5 periods while the middle one to 4 periods. The limit cycle observed in (10) can be encoded by the number of periods between the pulses. That shown in Figure 7a is $... - 4 - 4 - 4 - 5 - 4 - 4 - 4 - 5 - ...$ To describe such motions by a map we need a slightly corrected general shape of the map curve in Figure 6a. The result is shown in Figure 7c. The arrows indicate the trajectory corresponding to a four-period limit cycle attractor.

4 Chaotic oscillations

We expect that an appropriate choice of parameter values and feedback functions, $\Gamma(x, y)$ and $\Omega(x, y)$, yields a chaotic outcome of the system (3). As it is known chaotic oscillations are not possible with just the VdP element. On the other hand we would also like to have spike-burst behavior. For such purpose the choice of Ω made in Section 3 is not suitable. Thus, we choose Ω more complex than taken in equation (5). For illustration we take

$$\Gamma(u, I) = 0.18(1 - 5I - 10u), \Omega(u, I) = (1 - u)$$

and $m_1 = m_3 = 1, m_2 = 0.1, a = 0.01, l = 5, I = -0.06$. Figures 8a, b illustrate the time realization, $u(t)$, and the attractor of the system in the (x, u) representation. Here we approximate the *fast* motions of u by instantaneous jumps as done in Section 3, equations (6, 7), and analyze the system (10) for $\varepsilon_2 = 0.01$ within the regions F_0^+ and F_1^+ defined by equations (8).

To describe the attractor we have numerically constructed a Poincaré return map. Let us consider the map of the plane $u = a$ (Poincaré section) on itself by the trajectories of the attractor. It appears that the points are mapped closely to some curve as shown in Figure 9a. A linear fit gives

$$y = -0.21 + 0.024x.$$

It is taken approximately as a curve invariant under the map action and hence to describe the attractor the map may be one-dimensional. Iterating the curve points using (3) we obtain the one-dimensional map shown in Figure 9b. The attractor appears as a cluster of points very close to the map curve obtained. The map in Figure 9b does not have fixed points and consists of two continuous parts. The right one, approaching the bisector line from below, describes the *fast* jumps between the regions F_0^+ and F_1^+ of the phase space (Fig. 8). The left hand part describes *slow* motions in the region F_0^+ between the bursts of jumps. As shown in [19] the map in Figure 9b is chaotic and describes a chaotic attractor in the phase space of the system (3).

Thus, the system (3) when coupling relaxational and quasiharmonic oscillators displays a chaotic outcome in the form of "spiking-bursting" oscillations in the physiology jargon [5–9].

5 Conclusion

We have shown that a system composed of two nonlinearly coupled drastically different elements, one exhibiting smooth limit cycle oscillations and the other an excitable element displays a rich variety of attractors. These may be regular and chaotic. The phase space analysis of the system has shown the possibility to describe the attractors by one-dimensional Poincaré return maps.

The model studied (3), with a single excitation threshold, may exhibit pulses or spikes on top of quasiharmonic

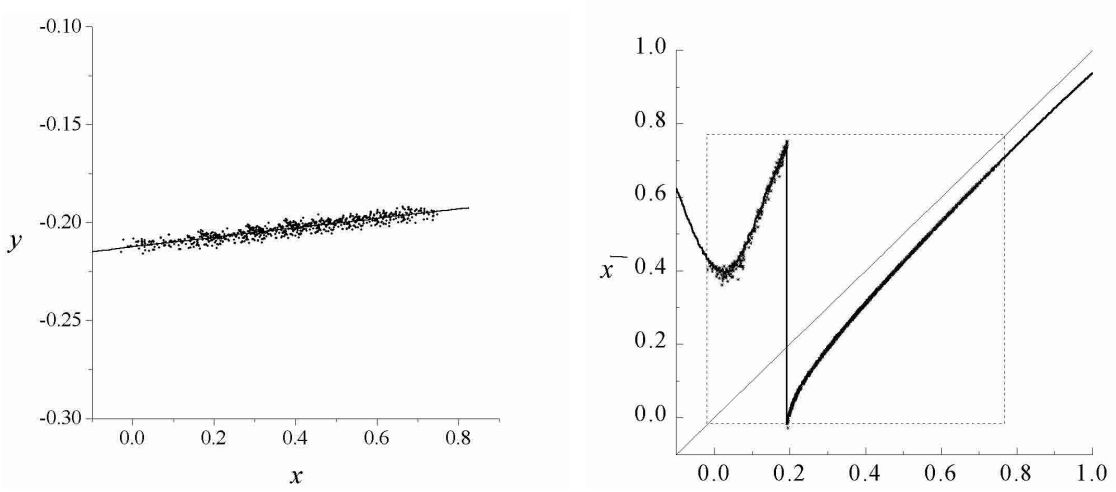

Fig. 9. (a) Intersection points of the trajectories of the attractor with the plane $u = a$ shown in Poincare plane section (x, y). The points approach the invariant curve. (b) 1D Poincaré map defined on the invariant curve. The dots indicate the trajectories of the attractor.

(limit cycle) oscillations. The inter-pulse interval is controlled by the values of the parameters of the system. Thus, such an oscillator may be of potential interest for driving feedback or feedforward loops or circuits in chemistry or biochemistry [1,2,4], in physiology [5–9] or in electronics [10] and in other engineering applications. Indeed, the composite system (3) defines well a generator with a single excitation threshold producing both a definite smooth rhythm, controllable pulses, chaotic behavior, and almost any combination, simple or complex, of pulses on top of the oscillations. For a very recent neurobiological application of the methodology here presented to account for the dynamics of (Inferior Olive) neurons with two excitability thresholds see reference [20].

Motivation for this research came from illuminating discussions with Prof. H. Haken, Prof. R. Llinas, Prof. L.O. Chua and Prof. A. Fernandez de Molina. This research has been supported by the BCH Foundation (Spain), by the Russian Foundation for Basic Research under Grant 97-02-16550, by the Program "Soros Post Graduate Students" under Grant a99-861 (Russia), by DGICYT (Spain) under Grant PB9-0599 and by the European Union under Grant FRB FM RX-CT96-10. V.I.N. benefited from a Sabbatical position at Instituto Pluridisciplinar, Universidad Complutense de Madrid.

We also wish to show our appreciation to an anonymous referee for comments that helped improving the presentation of our results.

References

1. S. Watanabe, S.H. Strogats, H.S.J. van der Zant, T.P. Orlando, Physica D **97**, 429 (1995).
2. Y. Kuramoto, *Chemical Oscillations, Waves and Turbulence* (Springer-Verlag, New York, 1984).
3. A. Goldbeter, *Biochemical oscillations and Cellular Rhythms* (Cambridge Unit. Press, Cambridge, 1996).
4. A.T. Winfree, *The Geometry of Biological Time* (Springer-Verlag, Berlin, 1980).
5. H. Haken, *Principles of Brain Functioning* (Springer-Verlag, Berlin, 1996).
6. H.D.I. Abarbanel, M.I. Rabinovich, A. Selverston, M.V. Bazhenov, R. Huerta, M.M. Sushchik, L.L. Rubchinskii, Phys. Usp. **39**, 337 (1996).
7. J.P. Welsh, R. Llinas, Progress Brain Res. **114**, 449 (1997).
8. R. Llinas, Y. Yarom, J. Physiol. **376**, 163 (1986).
9. L.S. Bernardo, R.E. Foster, Brain Res. Bull. **17**, 173 (1986).
10. *Chua's circuit: a Paradigm for Chaos*, edited by R.N. Madan (World Scientific, Singapore, 1993).
11. V.S. Afraimovich, V.I. Nekorkin, G.V. Osipov, V.D. Shalfeev, *Stability, structures and chaos in nonlinear synchronization networks* (World Scientific, Singapore, 1995).
12. A.A. Andronov, A.A. Vitt, S.E. Khaikin, *Theory of oscillations* (Pergamon, N.Y., 1966).
13. R. Fitz Hugh, Biophys. J. **1**, 445 (1961).
14. E.F. Mishenko, N.Kh. Rozov, *Diffential equations with small parameters and relaxation oscillations* (Plenum Press, New York, 1980).
15. N.N. Bogoliubov, Y.A. Mitropolsky, *Asymptotic methods in the theory of nonlinear oscillations* (Hindustan Publishers, New Delhi, 1961).
16. J. Guckenheimer, R. Holmes, *Nonlinear Oscillations, Dynamical Systems, and Bifurcations of Vector Fields* (Springer-Verlag, N.Y., 1983).
17. J.K. Hale, *Oscillations in Nonlinear Systems* (Mc Graw-Hill, N.Y., 1963).
18. Yu.A. Mitropolsky, O.B. Lykova, *Integral Manifolds in Nonlinear Mechanics* (Nauka, Moscow, 1973) (in Russian).
19. V.I. Nekorkin, V.B. Kazantsev, L.O. Chua, Int. J. Bifurcation Chaos **6**, 1295 (1996).
20. M.G. Velarde, V.I. Nekorkin, V.B. Kazantsev, V.I. Makarenko, R.R. Llinas, Neural Comp. (submitted).